

RESEARCH ARTICLE | DECEMBER 16 2024

Loss of bimolecular reactions in reaction–diffusion master equations is consistent with diffusion limited reaction kinetics in the mean field limit

Tina Subic ; Ivo F. Sbalzarini  



J. Chem. Phys. 161, 234107 (2024)

<https://doi.org/10.1063/5.0227527>



Articles You May Be Interested In

KoopmanLab: Machine learning for solving complex physics equations

APL Mach. Learn. (September 2023)

Experimental realization of a quantum classification: Bell state measurement via machine learning

APL Mach. Learn. (September 2023)



The Journal of Chemical Physics

Special Topics Open for Submissions

[Learn More](#)

Loss of bimolecular reactions in reaction–diffusion master equations is consistent with diffusion limited reaction kinetics in the mean field limit

Cite as: J. Chem. Phys. 161, 234107 (2024); doi: 10.1063/5.0227527

Submitted: 9 July 2024 • Accepted: 29 November 2024 •

Published Online: 16 December 2024



Tina Subic^{1,2,3,a)}  and Ivo F. Sbalzarini^{1,2,3,4,b)} 

AFFILIATIONS

¹ Faculty of Computer Science, Dresden University of Technology, Dresden, Germany

² Max Planck Institute of Molecular Cell Biology and Genetics, Dresden, Germany

³ Center for Systems Biology Dresden, Dresden, Germany

⁴ Cluster of Excellence Physics of Life, TU Dresden, Dresden, Germany

^{a)} Now at: Department of Computational and Systems Biology, University of Pittsburgh, Pittsburgh, PA 15213, USA.

^{b)} Author to whom correspondence should be addressed: sbalzarini@mpi-cbg.de

ABSTRACT

We show that the resolution-dependent loss of bimolecular reactions in spatiotemporal Reaction–Diffusion Master Equations (RDMEs) is in agreement with the mean-field Collins–Kimball (C–K) theory of diffusion-limited reaction kinetics. The RDME is a spatial generalization of the chemical master equation, which enables studying stochastic reaction dynamics in spatially heterogeneous systems. It uses a regular Cartesian grid to partition space into locally well-mixed reaction compartments and treats diffusion as a jump reaction between neighboring grid cells. As the chance for reactants to be in the same grid cell decreases for smaller cell widths, the RDME loses bimolecular reactions in finer grids. We show that for a single homo-bimolecular reaction, the mesh spacing can be interpreted as the reaction radius of a well-mixed C–K rate. Then, the bimolecular reaction loss is consistent with diffusion-limited kinetics in the mean-field steady state. In this interpretation, the constant in a bimolecular reaction propensity is no longer the macroscopic reaction rate but the rate of the ballistic C–K step. For the same grid resolution, different diffusion models in RDME, such as those based on finite differences and Gaussian jumps, represent different reaction radii.

© 2024 Author(s). All article content, except where otherwise noted, is licensed under a Creative Commons Attribution-NonCommercial-NoDerivs 4.0 International (CC BY-NC-ND) license (<https://creativecommons.org/licenses/by-nc-nd/4.0/>). <https://doi.org/10.1063/5.0227527>

I. INTRODUCTION

Diffusing and interacting molecules are the basis of chemical reactions. Confined to small spaces, or at low molecule count, chemical reactions are subject to intrinsic noise arising from the discreteness of molecules, the quantum nature of reactions, and the thermal Brownian motion of diffusion. This is typically the case in biological cells, where the interplay between stochastic reactions and diffusion has been shown to affect cellular dynamics.^{1–7} This allows cells to exploit intrinsic noise^{1–4} but may also require mechanisms to buffer noise.^{5–7}

Both the intrinsic noise and the distribution of molecules can be spatially heterogeneous in reaction–diffusion systems, even at steady state.⁸ Reaction–diffusion models have thus enabled describing cellular processes ranging from chemotaxis⁹ to cell polarization.^{10,11} It

is reasonable to assume that both spatial heterogeneity and stochasticity contribute to cellular processes, albeit to various degrees. For example, slow diffusion has been shown to lead to faster responses in signaling pathways due to more localized molecule concentrations,¹² and local fluctuations of molecules can have a significant effect on spatial patterning.¹³ Understanding these phenomena requires models that couple reaction stochasticity and spatial concentration gradients.

Stochastic reaction–diffusion models, such as Brownian Dynamics (BD)¹⁴ and the Reaction–Diffusion Master Equation (RDME),^{15,16} allow capturing the combined effect of stochasticity and spatial heterogeneity on reaction dynamics. BD represents individual molecules as particles that undergo random walk and can react with each other upon encounter within a given reaction radius. This provides an accurate microscopic description of the system but

leads to simulations with a computational cost that scales with the molecular population. The RDME generalizes the classic Chemical Master Equation (CME)¹⁷ to spatially inhomogeneous processes by partitioning space into locally well-mixed reaction volumes along a regular Cartesian grid^{15,18,19} or an unstructured mesh.^{20,21} In each grid cell, a CME models the local reaction dynamics, while diffusion is approximated with a continuous-time lattice random walk and implemented as a jump “reaction” from a cell to a neighboring cell, which need not be immediately adjacent.¹⁹ Tracking only the total number of molecules in each cell, rather than each molecule individually, the RDME provides a mesoscopic description of the system. While this renders the standard RDME unable to capture microscopic effects, like molecular crowding and volume exclusion, it typically results in a lower computational cost.

The lower computational cost of RDME simulations is exploited in several numerical algorithms²² and approximations.^{23–28} These Stochastic Simulation Algorithms (SSAs) simulate the jumps between grid cells as first-order reactions with a rate proportional to the molecular diffusivity and the grid-cell size. Therefore, they inherit the physical interpretation of the propensity constants from the CME. However, the subdivision of space by the RDME grid introduces additional reaction barriers. Indeed, two molecules can only react if they are in the same grid cell. Therefore, the RDME famously loses bimolecular reactions with finer partitioning of the reaction volume.^{18,29–31}

Loss of bimolecular reactions at higher spatial resolution is widely considered nonphysical and is often cited as the main limitation of RDME models.^{18,32–36} Correction factors to bimolecular propensities have been proposed to counter the dependence of bimolecular reaction frequencies on grid resolution.^{32–35} Using such corrected propensities, the RDME achieves the same steady state as a non-spatial CME. It has also been proposed to combine the RDME with microscopic methods^{36,37} to avoid the issue altogether. Alternatively, one can constrain the RDME to above a limit grid resolution, below which the loss becomes significant. This resolution limit represents a trade-off between the error of the spatial approximation of the diffusion process and the bimolecular reaction loss.^{22,30,31,34}

Interestingly, this limit grid-cell size is often derived from the concept of a reaction radius as used in BD. In fact, the subdivision of space into well-mixed sub-volumes is not introduced by the simulation algorithms but is an integral part of the RDME model itself. A comparison of RDME and BD models also showed a loss of bimolecular reactions in BD for decreasing reaction radius.¹⁸ This hints at the possibility that the bimolecular reaction loss in RDME might not be nonphysical and that there exists a relation between RDME grid resolution and BD reaction radius.

Formalizing the link between grid resolution and reaction radius, we propose a physical explanation for the loss of bimolecular reactions based on Collins–Kimball (C–K) theory of diffusion-limited reaction kinetics. In this theory, the macroscopic reaction rate depends on the molecular diffusivity, the reaction radius, and on what happens at the site of collision as encapsulated in the *ballistic rate*. In well-mixed CME models, it is known that the propensity constant derives from the macroscopic C–K rate.³⁸ Typically then, the (uncorrected) bimolecular propensities in RDME models are interpreted as C–K rates, and the grid resolution is chosen large enough to avoid significant loss of bimolecular reactions, yet small

enough to well approximate the diffusion.^{19,29–31,39} Here, we propose a different interpretation: the bimolecular propensities in RDME models, in contrast to the CME, represent the *ballistic rate alone*, and the grid resolution defines the reaction radius in addition to setting the spatial accuracy of the diffusion approximation.

Using this new interpretation, we show that two different RDME models—the standard model using finite differences for the jump reactions (fd-RDME) and a model using Gaussian jumps (GRDME)¹⁹—recapitulate the loss of bimolecular reactions expected from C–K diffusion-limited reaction kinetics. This suggests that the loss of bimolecular reactions in RDME models is physically consistent if the grid-cell size defines the reaction radius, analogous to how it is done in BD. In addition, the choice of diffusion model (GRDME vs fd-RDME) modulates the molecule size. GRDME offers an additional degree of freedom (the Gaussian jump neighborhood radius), which can be used to independently tune the reaction radius and the accuracy of the spatial diffusion approximation. Taken together, this suggests that the RDME can provide a correct mesoscopic model of C–K reaction kinetics, but that standard RDME (fd-RDME) may only be able to do so for reaction systems with a narrow spectrum of reaction radii and for a limited range of diffusion constants, whereas GRDME offers more flexibility.

II. RDME RECAPITULATES BIMOLECULAR REACTION LOSS OBSERVED IN DIFFUSION-LIMITED REACTION DYNAMICS

What is the dynamics of bimolecular reactions in a dilute solution without external mixing? A theoretical description of diffusion-limited reaction dynamics has been provided by Collins and Kimball⁴⁰ for three-dimensional systems. The theory considers the setting where molecules of species i diffuse with diffusivity D_i and collide with other molecules, resulting in a possible reaction. Consequently, two reactant molecules must first reach each other for a bimolecular reaction to occur, making a second-order reaction a two-step process. The *diffusion-limited reaction rate* k_{CK} (C and K stand for Collins and Kimball) of such a two-step process satisfies

$$\frac{1}{k_{CK}} = \frac{1}{k_b} + \frac{1}{k_d}, \quad (1)$$

where $k_d \equiv 4\pi\sigma D_\Sigma$ is the rate of the *diffusion* step and k_b is the rate of the *ballistic* step, encapsulating the dynamics at the collision site.³⁸ The reaction radius σ is the sum of the radii of two hard spheres, representing the two colliding molecules, and D_Σ is the diffusivity of the two reactant molecules relative to each other, $D_\Sigma = D_i + D_j$. The resulting overall rate of a bimolecular reaction in a dilute well-mixed solution thus is

$$k_{CK} = \frac{k_b k_d}{k_b + k_d} = \frac{4\pi\sigma D_\Sigma k_b}{4\pi\sigma D_\Sigma + k_b}. \quad (2)$$

Depending on which of the two steps is rate-limiting, one distinguishes two regimes: the *diffusional* regime with $k_{CK} \approx k_d$ and the *ballistic* regime with $k_{CK} \approx k_b$. Besides k_b , the sizes and diffusivities of the reactant molecules determine which regime is the system in.

How do diffusivity and size of molecules affect the dynamics of bimolecular reactions in solution? In the diffusional regime, $k_{CK} \approx 4\pi\sigma D_\Sigma$, and the overall reaction rate is proportional to the

diffusivity and size of the molecules. Smaller D_Σ leads to smaller k_{CK} because molecules encounter fewer reaction partners. Smaller σ also leads to smaller k_{CK} because smaller molecules occupy less volume and therefore have a smaller probability of collision. Smaller k_{CK} leads to fewer reactions, with all other things being equal.

How is diffusion-limited kinetics reflected in the CME? The CME describes how the probability of the reaction system being in a certain state \vec{s} evolves over time due to stochastic reactions. The instantaneous probability of a reaction happening is described by a propensity function⁴¹ a that depends on the state \vec{s} , the order of the reaction, the reaction volume size Ω , and the kinetic rate k . For a bimolecular reaction between molecules of species i and j , the propensity is $a = k \Omega^{-1} s_i s_j$. Gillespie³⁸ has rigorously shown that for *well-mixed and dilute* systems (that is, for the “non-spatial” CME), the reaction rate k in the bimolecular propensity is the diffusion-limited macroscopic rate k_{CK} . While the parameters that control the diffusion-limited dynamics (D , σ , and k_b) are not explicitly modeled by CME, they are implicitly accounted for in the value of the reaction rate.

To illustrate how reaction radius (σ) and diffusivity (D) affect the CME reaction dynamics through changing the bimolecular rate, we consider a reaction system with one homo-bimolecular reaction,



with state $s = \#X$, the number of molecules. Since both reactants are X and thus have the same diffusion coefficient D , the bimolecular reaction rate for diffusion-limited kinetics from Eq. (2) is

$$k_2 = k_{CK} = \frac{k_b 8\pi\sigma D}{k_b + 8\pi\sigma D}. \quad (4)$$

In Fig. 1(a), we show how the time average of the steady state $\langle s \rangle$ varies with σ and D . For large-enough D and σ , the system reaches the ballistic regime, where $\langle s \rangle$ no longer depends on D or σ . Thus, by changing the bimolecular rate constant k_2 in the CME as a function

of σ and D , the system experiences a loss of bimolecular reactions for decreased σ or D .

Unlike the CME, the RDME explicitly models diffusion. In grid-based RDME, the reaction volume Ω is decomposed using a Cartesian grid into M compartments of width h and volume h^d , where d is the spatial dimension (here $d = 3$ throughout). Each compartment p contains a sub-population \vec{s}^p of molecules all of which can react, and the bimolecular propensity between molecules i and j in a compartment becomes $a = k h^{-d} s_i^p s_j^p$. The diffusion of molecules across compartments is modeled as a first-order reaction in which a molecule in a compartment p is “converted” to a molecule of the same species in another compartment q with a rate $k_D = cD_i/h^2$, where c is a function of the diffusion model used.

The original formulation of RDME by Gardiner *et al.*,¹⁵ here referred to as fd-RDME, uses a finite-difference diffusion model for which $c = 1$ and the error for the spatial diffusion approximation scales as $O(h^2)$.^{19,39,42} Then, a molecule can jump to one of the $2d$ face-connected adjacent compartments. The total propensity for a molecule to jump anywhere in this neighborhood is

$$a_D^{\text{fd-RDME}} = 2d \frac{D}{h^2}. \quad (5)$$

In the GRDME, molecules can jump to a larger neighborhood, with a Gaussian rate proportional to the distance of the jump. Therefore, the GRDME has $c = \frac{h^d}{\epsilon'^2} \left(\frac{1}{4\pi\epsilon'^2} \right)^{\frac{d}{2}} \exp\left(-\frac{l^2}{4\epsilon'^2}\right)$, where l is the length of the jump and $\epsilon' \geq 1$ is an additional parameter that controls the radius of the Gaussian neighborhood. The error for the spatial diffusion approximation in GRDME scales as $O(\epsilon'^2 h^2)$. For a fixed h , the diffusion error scales as ϵ' as $O(\epsilon'^2)$.¹⁹ The total diffusional propensity for GRDME is

$$a_D^{\text{GRDME}} = \epsilon'^{-2} \frac{D}{h^2}. \quad (6)$$

In both grid-based RDME models, the bimolecular propensity and the number of compartments M scale with the space dimension d , whereas the diffusional propensity scales inversely quadratically

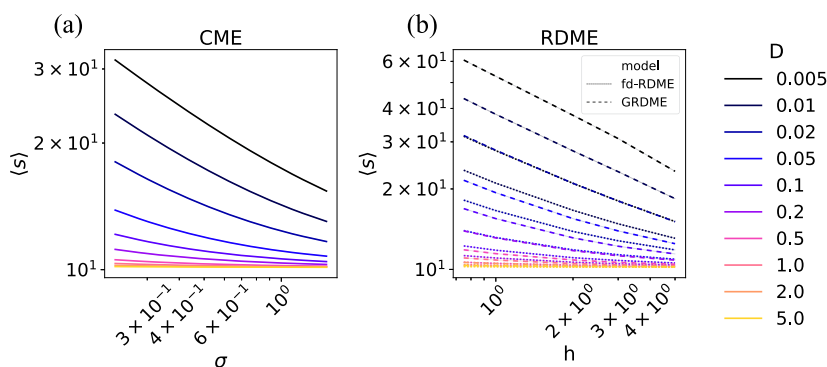


FIG. 1. Reaction loss in diffusion-limited CME resembles reaction loss in RDME. We show the time-average estimate of the steady-state number of molecules s of the reaction system in Eq. (3), modeled by the CME (a) and the RDME (b) for varying length scale [the diffusion-limited C-K reaction radius σ in the CME, see Eq. (2); the grid cell size h in the RDME]. The experiment is repeated for different diffusivities D , shown in color where the darkest hue represents the smallest D (color bar legend on the right). For RDME, we use two different diffusion models: fd-RDME (dotted lines) and GRDME (dashed lines); see the inset legend. Results are shown on a log-log scale. All simulation parameters are listed in Table II. The barely visible error bands (semi-transparent color) show the 95% confidence intervals of the time-averaged estimates.

with the grid spacing h . With decreasing h , the molecules explore smaller fractions of Ω and thus encounter fewer potential reaction partners. Hence, bimolecular reaction loss is also observed in grid-based RDME models, both when decreasing D and when decreasing h .

There were many dedicated efforts toward finding good or even optimal (in some sense) grid resolutions h for RDME, balancing the accuracy of diffusion approximation and the loss of bimolecular reactions.^{18,31–35} However, as shown in Fig. 1(a), also the CME with diffusion-limited C–K rates loses bimolecular reactions for decreasing reaction radii [note that in the bimolecular reaction in Eq. (3) is an annihilation reaction such that higher $\langle s \rangle$ indicates a stronger loss of bimolecular reactions]. This is akin to the trend observed in Fig. 1(b), which shows the extent of bimolecular reaction loss as a function of h for fd-RDME and GRDME. Both RDME models experience reaction loss for decreasing h , albeit to a different extent. This suggests that, rather than being a nonphysical consequence of grid partitioning, bimolecular reaction loss in RDME models could be due to the reaction system transitioning from the ballistic regime to the diffusion-limited regime.

The question then is whether the bimolecular reaction loss in RDME models is consistent with the C–K theory. RDMEs explicitly model diffusion as first-order jump reactions between compartments. Yet, diffusion is also encapsulated in the bimolecular propensity constant, which represents the diffusion-limited macroscopic reaction rate. This means that in the current interpretation of rates in RDME, diffusion is accounted for twice. Thus, we need to reexamine the physical interpretation of the rate constant of the bimolecular propensity in RDME. Furthermore, as σ and D go hand-in-hand in C–K dynamics, we cannot explicitly model one without accounting for the other. Thus, we propose an alternative interpretation of the reaction loss observed in RDME: the RDME models a reaction system in which the *observed* reaction dynamics is described by the diffusion-limited bimolecular (macroscopic) reaction rate k_{CK} , the bimolecular propensity constant k_2 is the ballistic rate k_b , and the grid resolution h sets the reaction radius σ .

III. GRID RESOLUTION DEFINES REACTION RADIUS

If the loss of bimolecular reactions in RDME can be explained by C–K theory, then one should be able to relate the reaction radius σ and the grid cell size h . We can estimate k_{CK} (the macroscopic

reaction rate) from the time-averaged steady-state concentration $\langle s \rangle$ and the birth rate k_1 by expressing k_{CK} from the steady-state solution of the deterministic rate equation of the reaction system in Eq. (3) as

$$k_{CK} = k_1 \left(\frac{\Omega}{\langle s \rangle} \right)^2. \quad (7)$$

C–K theory relates k_{CK} to σ . However, the resulting prediction may not represent the sum of the two molecule radii. We therefore refer to the length scale estimated from k_{CK} as σ^* as follows:

$$\sigma^* = \frac{k_{CK} k_2}{8(k_b \pi D - k_{CK} \pi D)}. \quad (8)$$

This predicts σ^* to vary with D and k_2 (hypothesized to represent k_b).

To see how σ^* depends on the system parameters, we compute the time average of the mean $\langle s \rangle$ (time interval $[T_{\text{start}}, T]$, see Table I) of the reaction system in Eq. (3) using fd-RDME and GRDME ($\epsilon' = 1$) for varying Ω , k_1 , and D , while keeping h fixed—see Table I. We expect to find two constant values for σ^* , one for each of the two models (fd-RDME and GRDME with $\epsilon = 1$). In Fig. 2(a), we plot σ^* obtained for each combination of k_1 and Ω over 100 independent repetitions of each simulation for the two models as a function of D . Indeed, σ^* remains constant when varying k_1 , Ω , or D . For a large D , the standard error in the average σ^* (over the 100 independent replicas) sharply increases. This happens because the system is no longer diffusion-limited such that $k_{CK} \approx k_b$ and $\langle s \rangle$ becomes independent of D . In the ballistic regime, σ^* becomes undetermined and can therefore not be estimated from simulations. This happens at lower D for fd-RDME than for GRDME.

Given that σ^* does not depend on the system parameters for a given, fixed h , does it depend on h ? We study this in simulations in which we vary k_b , D , and h —the complete set of parameters controlling k_{CK} according to Eq. (2). All simulation parameters are again listed in Table II, but we additionally vary $k_b \in \{0.125, 0.25, 0.5\}$. For each parameter combination, we compute σ^* from k_{CK} using Eqs. (7) and (8). We hypothesize that the bimolecular rate in RDME is the rate of the ballistic step k_b alone. Then, k_b is the independent parameter in the simulation, and not k_{CK} . We therefore measure k_{CK} in the simulations from k_1 and $\langle s \rangle$ using Eq. (7). From this, we

TABLE I. Parameter values used to generate time-averaged estimate of the reaction system in Eq. (3) for Fig. 2(a).

Birth rate	k_1	$1.715 \cdot 10^{-8}, 3.429 \cdot 10^{-8}, 6.859 \cdot 10^{-8}$
Bimolecular propensity rate	k_b	0.125, 0.25, 0.5
Cell width	h	2
Domain length	L	24, 30, 38
Domain volume	Ω	13 824, 27 000, 54 872
Diffusivity	D	$1 \cdot 10^m, 2 \cdot 10^m, 3 \cdot 10^m, 5 \cdot 10^m$ $m = -3, -2, -1, 0$
Simulation time	T	$2 \cdot 10^8$
Collection start point for $\langle s \rangle$	T_{start}	$5 \cdot 10^5$
Number of repetitions	n	100

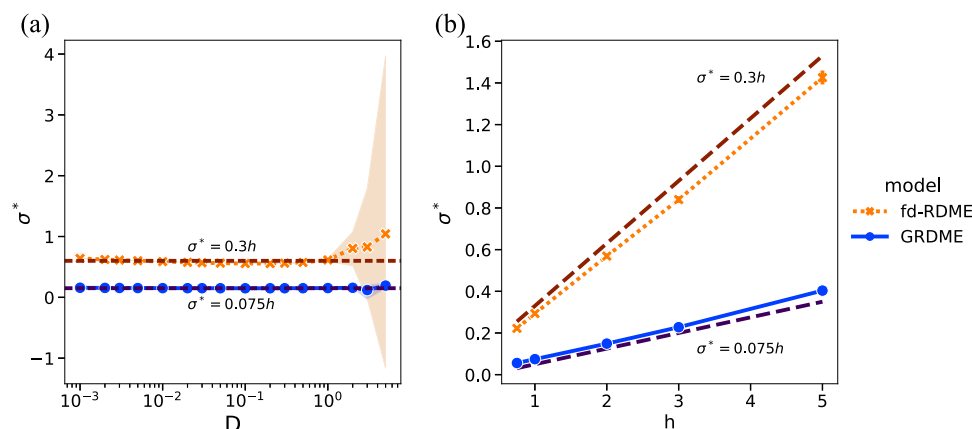


FIG. 2. Grid resolution sets the reaction radius. Estimated reaction radius σ^* for fd-RDME (orange dotted line) and GRDME, $\epsilon' = 1$ (blue solid line) as a function of diffusion constant D (a) and RDME grid resolution h (b). Dark orange dashed lines indicate $\sigma^* = 0.3h$ for fd-RDME, and dark blue dashed lines indicate $\sigma^* = 0.075h$ for GRDME. (a) Computed σ^* for each combination of parameters Ω and k_1 in Table I as a function of D on a logarithmic scale. The error bands (light shaded areas) show the 95% confidence interval over 100 independent repetitions of each stochastic simulation. The σ^* is the same for any combination of parameters for each of the two models and a fixed h . (b) Average σ^* for each trajectory across varying RDME cell width h using all combinations of parameters from Table II, except $D \geq 0.5$ since the reaction radius is undetermined in the ballistic regime. The 95% confidence bands are below the linewidth.

TABLE II. Parameter values used to solve the reaction system in Eq. (3) for Figs. 1, 2(b), and 3.

Birth rate	k_1	$3.429 \cdot 10^{-8}$
Bimolecular propensity rate	k_b	0.25
Reaction radius (for CME)	σ	50 log-spaced values in $[0.225, 1.5]$
Cell width (for RDME)	h	0.75, 1, 2, 3, 5
Domain length	L	30
Domain volume	Ω	27 000
Diffusivity	D	0.005, 0.01, 0.02, 0.05, 0.1, 0.2, 0.5, 1.0, 2.0, 5.0
Simulation time	T	$2 \cdot 10^8$
Collection start point for $\langle s \rangle$	T_{start}	$5 \cdot 10^5$
Number of repetitions	n	50

compute σ^* according to C-K theory using Eq. (8). Note that both Eqs. (7) and (8) are not explicit functions of h . A consistent emerging correlation between h and σ^* would therefore show that σ^* is set by h . Indeed, the results in Fig. 2(b) suggest a linear relation between σ^* and h across all tested simulation parameters, with $\sigma_{\text{GRDME}}^* = 0.075h$ and $\sigma_{\text{fd-RDME}}^* = 0.3h$. These pre-factors are the same as those found in Fig. 2(a) for the constant case. Thus, this is consistent evidence that σ^* is a linear function of h with a slope that depends only on the choice of the diffusion model.

If σ^* is a linear function of h , does h then represent the reaction radius in RDME models? If this is true, then fd-RDME and GRDME should both match the CME prediction in which the net effect of diffusion-limited kinetics is accounted for by using the bimolecular C-K rate from Eq. (4) at corresponding h and σ^* . The solid lines in Figs. 3(a) and 3(b) show the results of simulations with fd-RDME and GRDME, respectively, for different D (color) and h . The dashed lines show the results from the (non-spatial) CME, where the bimolecular rate was computed from σ^* and D

according to Eq. (4). Both RDME models closely match the CME results when using the corresponding σ^* from C-K theory, as can be seen in the small relative (to CME baseline) Mean Squared Error (MSE) of the two RDME models in Figs. 3(c) and 3(d). For small D , however, the error increases at larger h for GRDME. In Figs. 3(e) and 3(f), we show a sensitivity analysis, where we perturb the reaction radii in the CME baseline by a factor $\eta \in [0.5, 2.0]$, yielding $k_{\text{CK}} = k_b 8\pi \eta \sigma D / (k_b + 8\pi \eta \sigma D)$. The results show that the predictions are most sensitive to the setting of the reaction radius σ^* in the diffusion-limited regime, i.e., for smaller h and smaller D . For high D , the error barely depends on the perturbation to the reaction radius, as expected for the ballistic regime.

This suggests that the RDME models a diffusion-limited system, as we are able to predict the dynamics using the CME with a diffusion-limited bimolecular reaction rate, and the results are most sensitive in the diffusion-limited regime. In this case, the choice of h may be constrained beyond numerical considerations, as it represents a length scale of the system and therefore defines the chemical

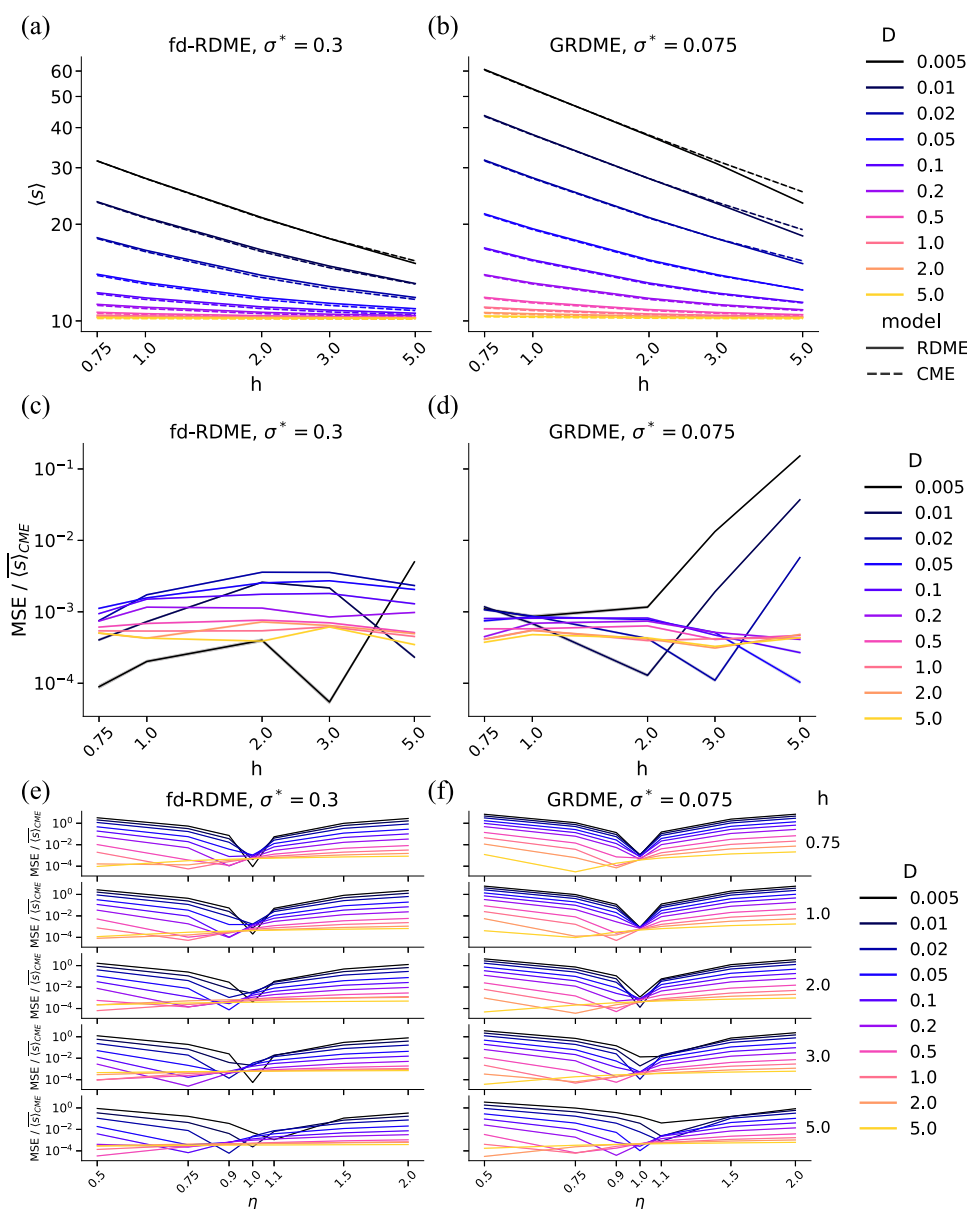


FIG. 3. RDME matches CME for diffusion-limited dynamics with the Collins–Kimball reaction radius. Steady-state number of molecules s in the reaction system from Eq. (3) as a function of RDME grid spacing h , computed as time averages of 50 independent RDME simulations (solid lines). The σ^* is determined from the linear relationship found in Fig. 2 and is then used to compute the bimolecular rate k_2 [Eq. (4)] of the corresponding CME (dashed lines). Results are shown for different D (colors, legend on the right) with the lowest value shown in the darkest hue. All simulation parameters are listed in Table II. The 95% confidence bands are shown as light shaded bands and are mostly thinner than the linewidth. (a) CME and fd-RDME with $\sigma^* = 0.3h$. (b) CME and GRDME with $\sigma^* = 0.075h$. (c) Normalized (to CME average) Mean Squared Error (MSE) between independent simulations of CME and fd-RDME with $\sigma^* = 0.3h$. (d) Normalized (to CME average) MSE between CME and GRDME with $\sigma^* = 0.075h$. (e) Sensitivity analysis of the normalized MSE between fd-RDME and a perturbed CME baseline with $\sigma^* = \eta \cdot 0.3h$ w.r.t. η . (f) Sensitivity analysis of the normalized MSE between GRDME and a perturbed CME baseline with $\sigma^* = \eta \cdot 0.075h$ w.r.t. η .

system in a similar manner as D and k_b do. Therefore, in the RDME, there is an implicit reaction radius for each h , which matches the macroscopic C–K dynamics.

IV. DIFFERENT DIFFUSION MODELS IN RDME ASSUME DIFFERENT REACTION RADII

GRDME and fd-RDME use different diffusion models with different diffusion propensities [cf. Eqs. (5) and (6)]. Consequentially, they model different σ^* for the same h . Concretely, reaction radii in the GRDME are smaller than in the fd-RDME. By extension,

varying the free parameter ϵ' in GRDME should also affect σ^* . Different σ^* in GRDME represent chemical systems with molecules of different sizes, enlarging the range of molecular sizes that can be modeled with a single h .

To better understand the relationship between σ^* and the diffusion model, we study how σ^* varies with ϵ' . The parameters used are listed in Table III. According to the total propensity of diffusion jumps for the GRDME [Eq. (6)], σ^* should vary with ϵ' as $O(\epsilon'^{-2})$.

The results in Fig. 4 confirm the expected scaling for $\epsilon' \geq 1$. For smaller ϵ' , however, σ^* slightly deviates from the theoretical line. Comparing the diffusional propensities of fd-RDME [Eq. (5)] and GRDME [Eq. (6)], we expect $\sigma_{\text{fd-RDME}}^* = 6\sigma_{\text{GRDME}, \epsilon'=1}^*$ for a

TABLE III. Parameter values used to generate the results in Fig. 4 for the reaction system in Eq. (3).

Birth rate	k_1	$3.429 \cdot 10^{-8}$
Bimolecular propensity rate	k_b	0.125, 0.25, 0.5
Cell width	h	0.5
Smoothing length	ε'	1.0, 1.2, 1.5, 1.7, 2, 3, 5
Domain length	L	30
Domain volume	Ω	27 000
Diffusivity	D	0.005, 0.01, 0.02, 0.05, 0.1, 0.2, 0.5, 1, 2, 5
Simulation time	T	10^8
Collection start point for $\langle s \rangle$	T_{start}	$5 \cdot 10^5$
Number of repetitions	n	50

three-dimensional reaction volume. However, in the numerical results in Fig. 2, $\sigma_{\text{fd-RDME}}^*$ is only about four times larger than $\sigma_{\text{GRDME}, \varepsilon'=1}^*$. How can we explain this? σ^* is the radius of a reaction sphere. The largest sphere that can fit inside a cubic grid cell of edge length h has radius $h/2$. This σ_{max}^* is indicated in Fig. 4 by the horizontal green dashed line. Extrapolating the theoretical line (black dashed) to $\varepsilon' < 1$, $\sigma^* = 0.5h$ should be reached at $\varepsilon' \approx 6^{-1/2}$. This is also the value of ε' for which GRDME has the same diffusional propensity as fd-RDME, implying that σ^* for fd-RDME is $h/2$ and

$$\sigma_{\text{GRDME}}^* = (\varepsilon' \sqrt{6})^{-2} \sigma_{\text{fd-RDME}}^* = \frac{1}{12} h \varepsilon'^{-2}. \quad (9)$$

However, the numerically computed $\sigma_{\text{fd-RDME}}^* = 0.3 h$ (orange dot in Fig. 4) is below $0.5h$. In addition, σ^* of GRDME with $\varepsilon' = 1$ also deviates from quadratic scaling, as it is slightly smaller than predicted by

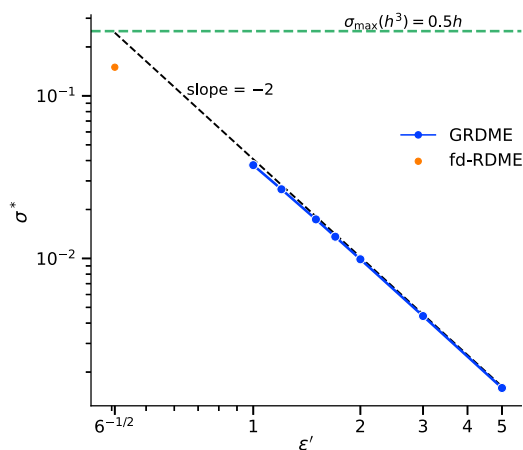


FIG. 4. Relationship between grid spacing h , GRDME parameter ε' , and reaction radius σ^* . Computed reaction radius σ^* for GRDME with varying smoothing length ε' (blue line with dots) and for fd-RDME (orange dot) on a log-log scale. We compute σ^* from the simulated steady-state number of molecules for the parameters in Table III. The σ^* of fd-RDME is at $\varepsilon' = \sqrt{6}^{-1}$, where the diffusional propensities of GRDME and fd-RDME coincide. The black dashed line indicates the theoretically expected scaling from Eq. (6). The horizontal green dashed line indicates the maximum possible $\sigma_{\text{max}}^* = h/2$ in a Cartesian grid of spacing h .

theory. It is therefore possible that the orange dot in Fig. 4 indeed lies on the sub-quadratically extrapolated blue line. The deviation might stem from the geometry of the mesh (Cartesian) or from the $\sigma \ll h$ restriction described in the literature^{30,31} (although this restriction has been derived assuming that the bimolecular propensity rate is k_{CK}). In any case, the difference between the numerically computed $\sigma_{\text{fd-RDME}}^*$ and the one predicted from quadratic scaling may explain why Smith and Grima¹⁸ were not able to match the reaction loss observed in BD to the reaction loss observed in the RDME when setting the reaction radius equal to the grid size h .

Nevertheless, the connection between σ^* and h elucidates an important modeling caveat of the fd-RDME: The reaction radius σ is defined as the sum of the radii of two colliding molecules, $\sigma = \sigma_i + \sigma_j$. This means that for different combinations of reactant species, it assumes different values. Nevertheless, fd-RDME models all reactions using a single grid spacing h , and hence a single $\sigma = \sigma^*$.

V. GRDME CAN MODEL MULTIPLE REACTION RADII WITH ONE FIXED GRID

If there exists only one bimolecular reaction in the system, either homo-bimolecular or hetero-bimolecular, then the system can be model by either fd-RDME or GRDME, since there is one well-defined σ from which to choose h . Using a fixed Cartesian grid, fd-RDME assumes all molecules in the system to have the same reaction radius. This can be problematic if there are multiple bimolecular reactions in the system with significantly different reaction radii. This is relaxed in GRDME, which offers an additional degree of freedom in ε' . Indeed, for a fixed grid spacing h , different ε' model different reaction radii as shown in Fig. 4.

From Eq. (9), the radius of an individual molecule, $\sigma_i = \frac{1}{2} \sigma^*$ (σ_i is the radius of an individual molecule and σ^* is the radius of the reaction sphere), in a homo-bimolecular reaction can be expressed as

$$\sigma_i = \frac{1}{24} h \varepsilon'^{-2}. \quad (10)$$

By definition, the reactant partners in homo-bimolecular reactions have the same size. However, this is generally not the case in hetero-bimolecular reactions. Unlike fd-RDME, GRDME can model a hetero-bimolecular reaction between two reactant molecules of different sizes by setting ε' separately for each chemical species

i and j . The reaction radius of the hetero-bimolecular reaction ($\sigma^* = \sigma_i + \sigma_j$) is thus

$$\sigma^* = \frac{1}{24}h \left(\frac{1}{\varepsilon_i'^2} + \frac{1}{\varepsilon_j'^2} \right). \quad (11)$$

To model a molecule of a given radius σ_i for a chosen, fixed h , the species-specific GRDME smoothing lengths ε_i' can thus be computed from the molecule radii as

$$\varepsilon_i' = \sqrt{\frac{h}{24\sigma_i}}. \quad (12)$$

Note here that σ_i is the radius of a molecule of species i and not the reaction radius σ^* . Consequently, the combination of ε_i' and h sets the size of the molecules of species i . This provides additional freedom in choosing h in the GRDME, e.g., to trade off computational cost and accuracy, which is not there for the fd-RDME. Moreover, it allows the GRDME to model bimolecular reactions with different σ^* using one fixed grid.

VI. ZERO-ORDER REACTIONS IMPOSE A LOWER DIFFUSIVITY LIMIT

The error of the diffusion models in fd-RDME and GRDME decreases with decreasing h when there are no reactions in the system.¹⁹ However, despite the improved accuracy of the diffusion model with decreasing h , in a system with reactions, the overall error in a RDME model increases again with decreasing h , due to the loss of bimolecular reactions. As shown above, the bimolecular reaction loss associated with decreasing h may be a consequence of an artificially decreased reaction radius. However, is there any other error associated with the grid spacing h ? And are there other limits of validity of the RDME?

Indeed, as we show in the following, such additional limits on h may exist for very large h and for very small D , for which grid-based RDMEs suffer from *insufficient* reaction loss if the reaction system contains zeroth-order (i.e., birth) reactions.

Consider again Fig. 2(b), which shows σ^* as a function of h on a log-log scale. For fd-RDME, the relation between σ^* and h appears to be slightly sub-linear. For GRDME, it becomes slightly super-linear for large h ($h \gtrsim 4$). Counterintuitively, this would mean that for large h , GRDME does not lose enough bimolecular reactions. To illustrate that, consider the extreme case $h = L$, for which we recover a non-spatial simulation. The system is then, by definition, in the ballistic regime with $k_2 = k_{\text{CK}} = k_b$ (note the ambiguity in the physical interpretation of the bimolecular propensity in this case) with no dependence on D and no loss of bimolecular reactions. Thus, we expect that for very large $h \approx L$, RDMEs may not adequately model diffusion-limited kinetics for small D .

This implies an error that is correlated with h and depends on the zeroth-order reactions in the system. The error can indeed be observed in Fig. 3, where GRDME (panel b) drops below the rate equations (RE, dashed line) for large h and small D (darker colors), implying insufficient loss of bimolecular reactions. The fd-RDME model (panel a) is slightly above the rate equations, consistent with the sub-linear scaling of its reaction radius σ^* . While we still do not know the source or the exact scaling of the error with h , both RDME

models have an error that is correlated with *increasing* grid-cell size h , whereas the error due to bimolecular reaction loss increases with *decreasing* h .^{30–37} The constraint from below on the ratio $\frac{L}{h}$ effectively provides an upper bound on the range of reaction radii in the system that can possibly be modeled with RDMEs.

Since the diffusion-limited reaction rate in Eq. (2) is symmetric with respect to reaction radius and diffusion constant, this also implies a limit on the diffusivity. To see this, consider the limit case $D \rightarrow 0$. One would then expect no bimolecular reaction to happen at all, and indeed $k_{\text{CK}} = 0$ for $D = 0$ [cf. Eq. (2)]. In a RDME model with $D = 0$, molecules never leave the grid cell they were created in. However, two molecules that happen to have been created in the same grid cell can still react. RDME models in which zeroth-order (birth) reactions can occur thus have a non-zero probability for bimolecular reactions to happen even at $D = 0$. Therefore, we anticipate an *insufficient* loss of bimolecular reactions in RDME models for small D .

How small can D be in a RDME model before these errors become dominant? For the reaction system from Eq. (3), $\langle s \rangle \rightarrow \infty$ for $D \rightarrow 0$, since no bimolecular reactions happen and molecules accumulate in the system forever. In a RDME model, as we have suggested above, the bimolecular rate represents k_b , which is independent of D . Therefore, $\langle s \rangle$ will remain finite, but the ratio k_b/k_{CK} by which the RDME over-estimates the bimolecular reactions diverges to infinity as $D \rightarrow 0$. For an infinite bimolecular reaction rate, the $\langle s \rangle$ in a discrete stochastic model converges to $s_\infty = 0.5$.⁴³ In a RDME model, the grid cells become independent of each other in the absence of diffusion. Therefore, with M grid cells, the limit molecular population is $\langle s \rangle_{\text{max}} = 0.5M$. This is the limit for very high bimolecular rates, which is the worst case for RDME when in reality no bimolecular reactions should occur.

The smallest D that can be represented in a RDME therefore is D that yields a k_{CK} with the same $\langle s \rangle_{\text{max}}$ as a sum of M independent grid cells of volume h^3 , namely

$$\langle s \rangle_{\text{max}} = \Omega \sqrt{\frac{k_1}{k_{\text{CK}}}} = 0.5 \frac{\Omega}{h^3} = 0.5M. \quad (13)$$

To find this lower limit on D , D_{min} , we use the rate for the diffusional regime $k_{\text{CK}} = 8\pi chD$, since we study the system for $D \rightarrow 0$. Instead of σ^* , we use ch for some constant $c > 0$, since σ^* is a linear function of h with slope depending on the diffusion model (cf. Fig. 2): c (fd-RDME) = 0.3, c (GRDME, $\varepsilon' = 1$) = 0.075, and c (GRDME, $\varepsilon' > 1$) = $\frac{1}{12}\varepsilon'^{-2}$. Substituting the resulting expression for k_{CK} into Eq. (13), we find for the reaction system from Eq. (3)

$$D_{\text{min}} = \frac{k_1 h^5}{2\pi c}. \quad (14)$$

Hence, D_{min} depends on the diffusion model, on the birth rate, and strongly on the grid resolution.⁴⁴ Importantly, the expression for D_{min} is specific to the reaction system. For example, the limit steady state of a reaction system similar to the system in Eq. (3) but with an additional first-order reaction $X \xrightarrow{k_3} \emptyset$ would be $s_\infty = h^3 k_1/k_3$ for $D \rightarrow 0$. This would result in a more permissive D_{min} .

We empirically confirm the above-mentioned expression for D_{min} for fd-RDME and GRDME ($\varepsilon' = 1$) in Fig. 5, where we plot the numerically computed $\langle s \rangle$ as a function of D (solid lines). We

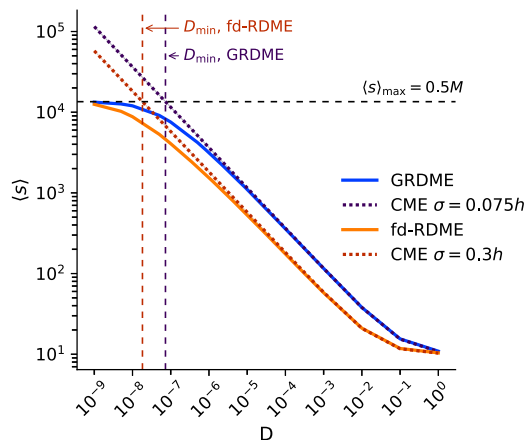


FIG. 5. For small D , RDME has *insufficient* bimolecular reaction loss. Time average of the steady-state number of molecules $\langle s \rangle$ in the reaction system from Eq. (3) as a function of the diffusivity D for fd-RDME (orange solid line), GRDME $\epsilon' = 1$ (blue solid line), and two CMEs with a diffusion-limited bimolecular rate k_{CK} , one with $\sigma = 0.3h$ (orange dotted line), corresponding to σ^* of fd-RDME, and the other with $\sigma = 0.075h$ (blue dotted line), corresponding to σ^* of GRDME. All simulation parameters are listed in Table IV. The horizontal black dashed line indicates the maximum possible value of $\langle s \rangle$, predicted by Eq. (13). The vertical dashed lines indicate D_{min} for fd-RDME and GRDME predicted by Eq. (14). The error bands (below the linewidth) show the 95% confidence interval over ten independent repetitions of each simulation.

compare this to the predictions from the CME with a bimolecular rate k_{CK} and $\sigma_{RDME}^* = 0.3$ and $\sigma_{GRDME}^* = 0.075$, respectively. All simulation parameters are summarized in Table IV. As $k_{CK} \rightarrow 0$, the steady state is reached at progressively later times, which is why we scale both the total simulation time T and the time T_{start} at which

we start collecting statistics for $\langle s \rangle$ accordingly. This ensures that all simulations reach the steady state before we start averaging $\langle s \rangle$.

We observe that both RDME models match the CME with k_{CK} well for larger D . However, $\langle s \rangle$ in the RDME models asymptotes at the maximum from Eq. (13) (indicated by a horizontal black dashed line), whereas it continues to increase for the CME. The D_{min} from Eq. (14) are indicated by vertical dashed lines (orange for fd-RDME and blue for GRDME). For both models, the CME predictions cross the line $\langle s \rangle_{max} = 0.5M$ exactly where predicted by D_{min} . This shows that in the presence of zeroth-order reactions, a D_{min} exists for both RDME models and that it is defined by the steady state of M independent reaction volumes of size h^3 .

VII. DISCUSSION AND CONCLUSION

We have shown that for a minimal bimolecular reaction system, one can linearly map the grid resolution of a RDME model to an effective reaction radius that recovers the well-mixed Collins–Kimball (C–K) rate in the mean-field limit. This suggests that RDME models, relying on a regular Cartesian grid, interpret the grid spacing as a reaction radius, in addition to it defining the accuracy of the spatial diffusion model. Then, the bimolecular propensity represents the rate of the *ballistic step alone* of diffusion-limited kinetics. This renders the bimolecular reaction loss in RDMEs consistent with the C–K theory of diffusion-limited reaction kinetics in three dimensions. In this interpretation, the grid resolution below which the model begins to lose bimolecular reactions is not a limit of validity of the RDME itself but rather corresponds to the reaction radius at which the system transitions from the ballistic to the diffusion-limited regime.

The RDME correctly models kinetics also in the diffusion-limited regime, where it coincides with the CME using the C–K rate. Nevertheless, a limit of validity for the RDME exists for systems that contain zeroth-order (birth) reactions. This limit, however, is a

TABLE IV. Parameter values used to generate the results in Fig. 5 for the reaction system in Eq. (3).

Birth rate	k_1	$3.429 \cdot 10^{-8}$
Bimolecular propensity rate	k_b	0.25
Diffusivity	D	$10^{-9}, 5 \cdot 10^{-9}, 10^{-8}, 5 \cdot 10^{-8}, 10^{-7}, 5 \cdot 10^{-7}, 10^{-6}, 10^{-5}, 5 \cdot 10^{-5}, 10^{-4}, 10^{-3}, 10^{-2}, 10^{-1}, 10^0$
Estimated reaction radius, GRDME	σ_{GRDME}^*	0.075
Estimated reaction radius, fd-RDME	$\sigma_{fd-RDME}^*$	0.3
Collins–Kimball reaction rate	k_{CK}	$\frac{k_b 8\pi\sigma^* D}{k_b + 8\pi\sigma^* D}$
Cell width	h	1
Domain length	L	30
Domain volume	Ω	27 000
Number of cells	M	$\Omega/h = 27\,000$
Simulation time	T	$10^7 \sqrt{\frac{k_b}{k_{CK}}}$
Collection start point for $\langle s \rangle$	T_{start}	$10^5 \sqrt{\frac{k_b}{k_{CK}}}$
Number of repetitions	n	10

lower limit on the diffusion constant, rather than a limit on the grid resolution. Indeed, for a given grid resolution, RDME models allow two molecules in the same grid cell to react even for zero diffusivity. This is because the diffusion constant in a RDME model controls the jump rate of molecules between grid cells but has no influence on the reaction kinetics within a cell. For very small diffusivity, RDME models thus become nonphysical, as they are losing *too few* bimolecular reactions. Below this lower diffusivity limit, the overall dynamics is better represented by an ensemble of independent well-mixed reaction systems.

Above the limit diffusivity, the choice of grid resolution in a RDME model defines the reaction radius σ^* . This is related to the radius σ of the sphere occupied by a pair of reactant molecules, but the two are not identical. Rather, the RDME σ^* , as defined by the grid resolution, can be interpreted as the radius of a sphere within which diffusion does not affect the reaction kinetics. Therefore, the reaction radius as used in Brownian dynamics methods is not the same as the reaction radius set by the grid resolution of a RDME model. Nevertheless, RDME models do assume a reaction radius. On-lattice models, such as RDME, therefore do not avoid the need for setting appropriate reaction radii. In practice, however, on-lattice approaches are often chosen precisely to avoid having to know microscopic system parameters. Our results point toward a possibility that on-lattice and off-lattice approaches may not be all that different in this regard, and that GRDME might potentially be a more expressive mesoscopic model than fd-RDME.

The key to setting the correct reaction radius in a RDME model is how σ^* scales with grid resolution h . As we have shown, this scaling is linear with a slope that only depends on the diffusion model used by the RDME. Since σ^* is smaller than h , consistent with the picture that multiple reactant pairs can simultaneously be within the same grid cell, diffusion within a grid cell should also be modeled but is neglected by RDMEs. This is why RDMEs are not able to correctly capture the dynamics for very small diffusion constants. The slower the scaling of σ^* with h , the more pronounced this error. This is why GRDME has a larger minimum diffusivity limit than fd-RDME. Neither fd-RDME nor GRDME, however, is physically consistent for very small diffusion constants below the limit we derived here.

An important difference between fd-RDME and GRDME is that GRDME possesses an additional parameter, the width ε' of the Gaussian jump kernel. As we have shown here, it is the combination of h and ε' that sets the reaction radius in GRDME. This enables GRDME to model different bimolecular reactions, with different reaction radii, using one grid resolution but species-specific ε' . It also allows the grid resolution h to be chosen according to the spatial diffusion accuracy desired, while the ε' can be chosen independently to match the reaction radii. This flexibility is not possible with fd-RDME, where one h sets the diffusion approximation accuracy as well as all reaction radii, such that, according to the present interpretation, all bimolecular reactions in a system must have similar reaction radii that are moreover compatible with the diffusion error.

While our results may appear to limit the use of RDME models, we would like to point out that the limiting h derived here is typically 5–10 times smaller than the lower limit for h proposed in previous studies. In particular, the consensus of previous studies is that h should be at least an order of magnitude larger than

the reaction radius.^{30,31,34} The interpretation provided in this work, therefore, would suggest a smaller h , improving at the same time also the accuracy of the diffusion approximation. We therefore believe that the present work might in fact extend the range of applicability and validity of RDME models.

Physical consistency for multiple bimolecular reactions on a single fd-RDME grid can potentially be restored by applying correction factors to bimolecular propensities.^{32–35} However, in light of the present results, the premise on which some of these factors were derived might need to be reconsidered. Some correction schemes aim to avoid the loss of bimolecular reactions altogether, which might not correctly model diffusion-limited kinetics. Indeed, using propensity correction, the steady state of the system remains constant for all grid resolutions above a certain validity limit of the correction scheme. Below this limit, the propensity-corrected system experiences a sudden and complete loss of bimolecular reactions.³² In the interpretation we proposed here, this means that propensity correction schemes increase the ballistic rate k_b to prevent the system from becoming diffusion-limited. Below their validity limit, the system is entirely diffusional, and the kinetics of the ballistic step no longer contribute to the dynamics. Propensity correction therefore models diffusion-limited kinetics only in the range of grid resolutions between the onset of bimolecular reaction loss in the uncorrected system and the validity limit of the correction scheme.

We have considered two different RDME models that use Cartesian grids, fd-RDME and GRDME. Comparing their different diffusion models was instrumental in understanding the physical interpretation of their parameters and establishing the correspondence with the C–K theory for diffusion-limited kinetics. Our considerations were, however, limited to three-dimensional reaction volumes, as the C–K theory only holds there. Moreover, we were limited to the case where a single, spatially isotropic and uniform grid resolution h characterizes the model. Future work could try to analyze spatially adaptive RDME models or models that use an unstructured grid, such as URDME.^{20,21} For those models, theoretical results are likely harder to come by, but numerical simulations might provide insight.

Based on the present results, future work could also try to improve the consistency of RDME at small diffusivities. The diffusivity limit derived here mainly stems from the design of zeroth-order reactions in current RDME models. The RDME model for zeroth-order reactions could be improved, e.g., by localizing zeroth-order reactions to the grid cell boundaries such that newly created molecules first require a diffusion event to enter any cell. This would prevent two molecules from being created within a distance of σ^* and ensure that there are no bimolecular reactions when there is no diffusion. Another approach could be to restrict zeroth-order reactions to empty grid cells or scale their propensities with the void fraction of the cell. This could eventually reconcile the RDME theory with models such as vRDME⁴⁵ and SPT-RDME⁴⁶ that account for finite-size effects of the reacting particles. In either case, one would need to ensure that the new model improves physical consistency with diffusion-limited kinetics. For example, vRDME uses an effective molecule diameter to model volume-exclusion effects in crowded systems. This parameter could not yet be linked to actual microscopic quantities, because the analysis in Ref. 45 was done in two dimensions, whereas C–K theory only holds for

three-dimensional systems. Going forward, it would be interesting to study the relationship between the reaction radius and volume exclusion effects by extending vRDME to three dimensions or by extending C–K theory to two dimensions.

Indeed, the role of the reaction radius in two-dimensional kinetics is an exciting and important question, for example for surface and interface systems. The kinetics of reaction loss in two dimensions differs fundamentally from that in three dimensions. In particular, in two dimensions, bimolecular reaction loss appears constant across all values of h , but instead seems to depend on the ratio between the bimolecular reaction rate and the diffusivity, as previously shown [Eq. (12) and Fig. 4(a) in Ref. 19]. Perhaps then, h can be set more freely in two-dimensional systems. However, this is speculation at this point, and further research is needed to understand the relationship between the reaction radius, grid resolution, and kinetics in two dimensions.

Interestingly, our interpretation of the RDME parameters shares similarities with the approach taken in convergent RDME (cRDME) models,³⁶ which are on-lattice RDME models of Doi's microscopic description. In addition, the cRDME uses the ballistic rate k_b as the bimolecular propensity. This similarity between our interpretation and the cRDME design points at the possible existence of a general mapping between microscopic system parameters and on-lattice master equation models.

It is important to keep in mind, though, that the present conclusions and interpretation were reached by comparing only the first moment of the RDME with the well-mixed CME for the simplest possible bimolecular reaction system at steady state. We considered this minimal model because it is theoretically tractable and its low-dimensional parameter space allowed for exhaustive numerical exploration. However, many open questions remain. For example, does a similar limit on h also exist for the time-dependent error before reaching the steady state? Is there an “optimal” value for h that minimizes the overall error in a RDME model? Would the conclusions still hold when other statistics are compared? Are there cases when fd-RDME cannot provide reasonable approximations at all, due to a spectrum of different reaction radii being present in the system? How could one calibrate RDME directly to a microscopic C–K model? Can the same principle be extended to two-dimensional systems, where the C–K theory does not exist? It is therefore clear that the present study is only a first step, possibly raising more questions than providing answers.

Despite these limitations, we suggested an alternative interpretation of the RDME model parameters in terms of microscopic quantities. This could effectively extend the utility of RDME models to regimes previously considered unattainable. More importantly, though, the microscopic reinterpretation of the model parameters allows for exploring the interplay between stochasticity and spatial heterogeneity in the diffusion-limited regime, as often found in biological cells.

ACKNOWLEDGMENTS

This work was funded in part by the German Research Foundation (DFG, Deutsche Forschungsgemeinschaft) under Code No. SB/53-1-1. We thank the anonymous reviewers for their constructive suggestions.

AUTHOR DECLARATIONS

Conflict of Interest

The authors have no conflicts to disclose.

Author Contributions

Tina Subic: Conceptualization (equal); Data curation (lead); Formal analysis (equal); Investigation (equal); Methodology (equal); Software (lead); Validation (lead); Visualization (lead); Writing – original draft (lead); Writing – review & editing (supporting). **Ivo F. Szbalzarini:** Conceptualization (equal); Formal analysis (equal); Funding acquisition (lead); Investigation (equal); Methodology (equal); Project administration (lead); Resources (lead); Supervision (lead); Validation (supporting); Visualization (supporting); Writing – original draft (supporting); Writing – review & editing (lead).

DATA AVAILABILITY

The data that support the findings of this study are openly available at <https://git.mpi-cbg.de/MOSAIC/GRDME>.

REFERENCES

- 1 J. Paulsson, O. G. Berg, and M. Ehrenberg, *Proc. Natl. Acad. Sci. U. S. A.* **97**, 7148 (2000).
- 2 J. M. G. Vilar, H. Y. Kueh, N. Barkai, and S. Leibler, *Proc. Natl. Acad. Sci. U. S. A.* **99**, 5988 (2002).
- 3 A. Eldar and M. B. Elowitz, *Nature* **467**, 167 (2010).
- 4 A. Gupta, B. Hepp, and M. Khammash, *Cell Syst.* **3**, 521 (2016).
- 5 C. A. Weber and C. Zechner, *Phys. Today* **74**(6), 38 (2021).
- 6 C. Briat, A. Gupta, and M. Khammash, *Cell Syst.* **2**, 15 (2016).
- 7 J. A. Riback and C. P. Brangwynne, *Science* **367**, 364 (2020).
- 8 A. M. Turing, *Philos. Trans. R. Soc., B* **237**, 37 (1952).
- 9 M. Onsum and C. V. Rao, *PLoS Comput. Biol.* **3**, e36 (2007).
- 10 N. W. Goehring, P. K. Trong, J. S. Bois, D. Chowdhury, E. M. Nicola, A. A. Hyman, and S. W. Grill, *Science* **334**, 1137 (2011).
- 11 T. Freisinger, B. Klünder, J. Johnson, N. Müller, G. Pichler, G. Beck, M. Costanzo, C. Boone, R. A. Cerione, E. Frey, and R. Wedlich-Söldner, *Nat. Commun.* **4**, 1807 (2013).
- 12 K. Takahashi, S. Tănase-Nicola, and P. R. ten Wolde, *Proc. Natl. Acad. Sci. U. S. A.* **107**, 2473 (2010).
- 13 D. Fange and J. Elf, *PLoS Comput. Biol.* **2**, 637 (2006).
- 14 J. Lipková, K. C. Zygalakis, S. J. Chapman, and R. Erban, *SIAM J. Appl. Math.* **71**, 714 (2011).
- 15 C. W. Gardiner, K. J. McNeil, D. F. Walls, and I. S. Matheson, *J. Stat. Phys.* **14**, 307 (1976).
- 16 S. Smith and R. Grima, *Phys. Rev. E* **93**, 052135 (2016).
- 17 D. T. Gillespie, *J. Phys. Chem.* **81**, 2340 (1977).
- 18 S. Smith and R. Grima, *Bull. Math. Biol.* **81**, 2960 (2018).
- 19 T. Subic and I. F. Szbalzarini, *J. Chem. Phys.* **157**, 194110 (2022).
- 20 S. Engblom, L. Ferm, A. Hellander, and P. Lötstedt, *SIAM J. Sci. Comput.* **31**, 1774 (2009).
- 21 B. Drawert, S. Engblom, and A. Hellander, *BMC Syst. Biol.* **6**, 76 (2012).
- 22 J. Elf and M. Ehrenberg, *Syst. Biol.* **1**, 230 (2004).
- 23 T. T. Marquez-Lago and K. Burrage, *J. Chem. Phys.* **127**, 104101 (2007).
- 24 S. Lampoudi, D. T. Gillespie, and L. R. Petzold, *J. Chem. Phys.* **130**, 094104 (2009).
- 25 B. Drawert, M. J. Lawson, L. Petzold, and M. Khammash, *J. Chem. Phys.* **132**, 074101 (2010).
- 26 J. Fu, S. Wu, H. Li, and L. Petzold, *J. Comput. Phys.* **274**, 524 (2014).

- ²⁷E. Roberts, J. E. Stone, and Z. Luthey-Schulten, *J. Comput. Chem.* **34**, 245 (2013).
- ²⁸M. J. Hallock, J. E. Stone, E. Roberts, C. Fry, and Z. Luthey-Schulten, *Parallel Comput.* **40**, 86 (2014).
- ²⁹S. A. Isaacson and C. S. Peskin, *SIAM J. Sci. Comput.* **28**, 47 (2006).
- ³⁰S. A. Isaacson, *SIAM J. Appl. Math.* **70**, 77 (2009).
- ³¹D. T. Gillespie, L. R. Petzold, and E. Seitaridou, *J. Chem. Phys.* **140**, 054111 (2014).
- ³²R. Erban and S. J. Chapman, *Phys. Biol.* **6**, 046001 (2009).
- ³³D. Fange, O. G. Berg, P. Sjöberg, and J. Elf, *Proc. Natl. Acad. Sci. U. S. A.* **107**, 19820 (2010).
- ³⁴S. Hellander, A. Hellander, and L. Petzold, *Phys. Rev. E* **85**, 042901 (2012).
- ³⁵S. Hellander, A. Hellander, and L. Petzold, *Phys. Rev. E* **91**, 023312 (2015).
- ³⁶S. A. Isaacson, *J. Chem. Phys.* **139**, 054101 (2013).
- ³⁷A. Hellander, S. Hellander, and P. Lötstedt, *Multiscale Model. Simul.* **10**, 585 (2012).
- ³⁸D. T. Gillespie, *J. Chem. Phys.* **131**, 164109 (2009).
- ³⁹S. A. Isaacson and D. Isaacson, *Phys. Rev. E* **80**, 066106 (2009).
- ⁴⁰F. C. Collins and G. E. Kimball, *J. Colloid Sci.* **4**, 425 (1949).
- ⁴¹D. T. Gillespie, *Physica A* **188**, 404 (1992).
- ⁴²D. Bernstein, *Phys. Rev. E* **71**, 041103 (2005).
- ⁴³The reaction $X + X \xrightarrow{k_2} \emptyset$ requires two reaction partners. Starting from $s = 0$, the first bimolecular reaction will only occur after at least two birth reactions ($\emptyset \xrightarrow{k_1} X$). Before reaching $s = 2$, the system will spend on average half of the time at $s = 0$ and half of the time at $s = 1$. Once $s = 2$, a bimolecular reaction brings the system back to $s = 0$. The larger the k_2 , the faster this happens, and the closer the system is to the limit $s_\infty = 0.5$.
- ⁴⁴This result can also be interpreted as a limit for h , $h_{\min} = (2\pi cD/k_1)^{1/5}$. While we are not yet able to physically interpret this limit, it varies little over a broad range of parameters. For example, for the reaction parameters in Table IV and varying $10^{-3} < D < 10^3$, the limit varies between $0.005 < h_{\min} < 0.090$.
- ⁴⁵C. Cianci, S. Smith, and R. Grima, *J. Chem. Phys.* **144**, 084101 (2016).
- ⁴⁶C. Cianci, S. Smith, and R. Grima, *Phys. Rev. E* **95**, 052118 (2017).